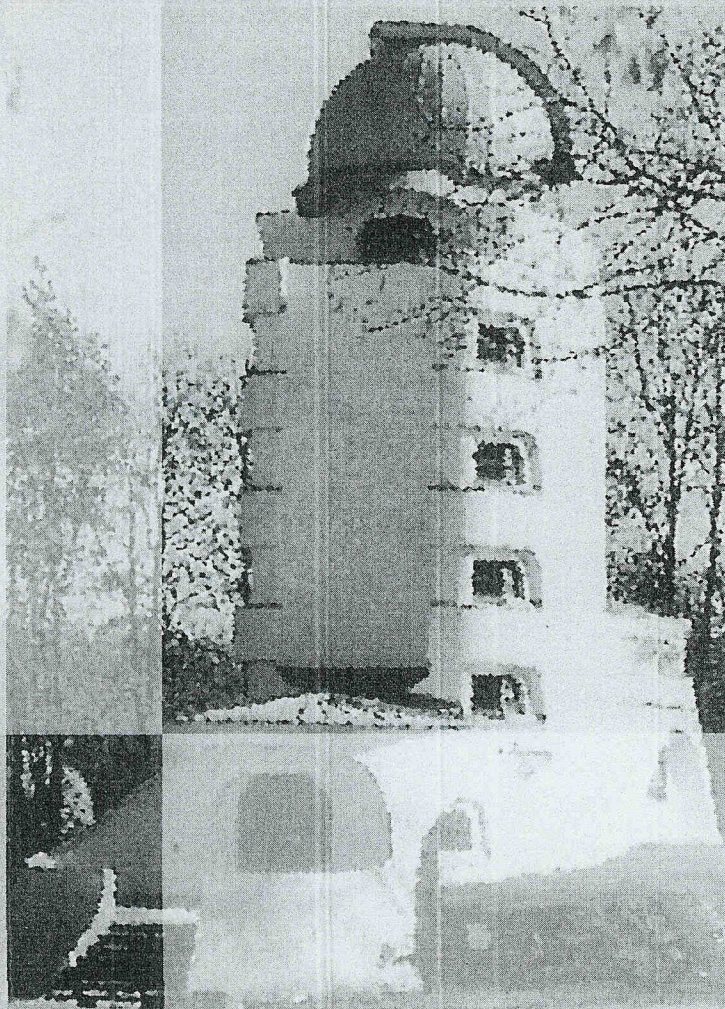


A. Ansmann
R. Neuber
P. Rairoux
U. Wandinger (Eds.)

Advances in Atmospheric Remote Sensing with Lidar



Selected Papers
of the
18th International
Laser Radar Conference
(ILRC),
Berlin, 22–26 July 1996



Springer

NDSC Intercomparison of Stratospheric Aerosol Processing Algorithms

W. Steinbrecht¹, H. Jäger², A. Adriani, G. di Donfrancesco, J. Barnes,
G. Beyerle, R. Neuber, C. David, S. Godin, D. Donovan, A.I. Carswell,
M. Gross, T. McGee, F. Masci, A. D'Altorio, V. Rizi, G. Visconti,
I.S. McDermid, G. Megie, A. Mielke, B. Stein, C. Wedekind, T. Nagai,
O. Uchino, H. Nakane, M. Osborn, D. Winker,

¹ DWD, Met. Obs. Hohenpeissenberg, Germany. wolfgang@mohp.dwd.d400.de

² IFU, Garmisch-Partenkirchen, Germany. jaeger@ifu.fhg.de

Abstract. Scattering ratios R processed from the same rawdata at 353 and 532 nm by different lidar groups agree within about 10 % for high and within about 4 % for low aerosol loading. In the main layer aerosol backscatter coefficients agree within about 30 % for high and within about 40 % for low aerosol loading

An intercomparison of algorithms used by different lidar groups for retrieving optical parameters of stratospheric aerosol was organized as part of the Network for the Detection of Stratospheric Change (NDSC). Using their individual algorithms all participating groups processed a set of 6 lidar signals recorded (photon counting) under conditions of high (18/19 1 1992), moderate (02/03 8 1993) and

Table 1. Participating groups and their processing algorithms.

group	method	density extrapolation
AWI, Potsdam	Klett, fixed α/β	no extrapol. above sonde
CNR, Frascati	iterative, 532: $\alpha = f(\beta)$ 353: fixed α/β	density from NMC
CNRS, Paris	Klett, fixed α/β	p and T gradient from MAP 85
DWD, Hohenpeissenberg	iterative, $\alpha = f(\beta)$	merge T with Lidar or CIRA 86
FU, Berlin	Klett, fixed α/β	density from US-Standard, normalized at sonde top
IFU, Garmisch	iterative, profile for α/β	exponential density extrapol.
MRI, Tsukuba	Fernald (Klett), fixed α/β	density from US-Standard, normalized at sonde top
NASA, Goddard	Fernald (Klett), fixed α/β normally use Raman channel	exponential density extrapol.
NASA, Langley	iterative fixed α/β	CIRA 86 density
NIES, Tsukuba	Fernald (Klett), fixed α/β	gradually shift from sonde to CIRA 86
NOAA, Mauna Loa	Fernald (Klett), fixed α/β	exponential density extrapol. max. 2 km above sonde
University, L'Aquila	iterative, fixed α/β	use standard atmosphere
York University/ISTS, Toronto	iterative, $\alpha = f(\beta)$	linear extrapol. of T or merge with T from lidar

low aerosol loading (19/20 9 1994) at IFU, Garmisch (532 nm) and at DWD, Hohenpeissenberg (353 nm). Instrumental effects, like counter saturation, neutral density filters etc. were already corrected for. Atmospheric density profiles were given in the form of significant levels from radio sondes launched about 80 km northeast.

Figures 1 and 2 show results at 353 nm and 532 nm for the case of high (left panels) and low (right panels) aerosol loading. For high loading differences between derived scattering ratios R are of the order of $\pm 5\%$ at 353 and 532 nm. Above the aerosol layer normalization is the main cause of differences, at the bottom of the aerosol layer the way aerosol extinction is accounted for causes additional spread in the results. For the low aerosol case deviations of R from the average $\langle R \rangle$ are smaller than ± 1 and 2 % for 353 and 532 nm respectively. Main cause is the normalization, differences in optical depth estimation do not contribute significantly.

References

1. Fernald, F.G., Herman, B.F., Reagan, J.A.: Determination of Aerosol Height Distributions by Lidar. *J. Appl. Met.* **11** (1972) 482–490
2. Klett, J.D.: Stable Analytical Inversion Solution for Processing Lidar Returns. *Appl. Opt.* **20** (1981) 211–220 and Klett, J.D.: Lidar Inversion with Variable Backscatter/Extinction Ratios. *Appl. Opt.* **24** (1985) 1638–1643
3. Russell, P.R., Swissler, T.J., McCormick, M.P.: Methodology for Error Analysis and Simulation of Lidar Aerosol Measurements. *Appl. Opt.* **18** (1979) 3783–3797.

Table 2. Integrated backscatter $\int \beta [\text{sr}^{-1}]$, extinction to backscatter ratio $\alpha/\beta [\text{sr}]$, optical density τ and normalization altitude $z_o [\text{km}]$.

group	532 nm, 18/19 Jan. 1992				353 nm, 18/19 Jan. 1992			
	$\int_{11}^{30} \beta$	α/β	$\tau(11,30)$	z_o	$\int_{14}^{30} \beta$	α/β	$\tau(14,30)$	z_o
AWI, Potsdam	3.058e-3	40.0	1.224e-1	25-29	3.507e-3	30.0	1.053e-1	25-29
CNR, Frascati	3.395e-3	36.1*	1.225e-1	35-40	4.623e-3	25.0	1.139e-1	34-40
CNRS, Paris	3.256e-3	40.0	1.319e-1	29	3.249e-3	40.0	1.278e-1	29.3
DWD, MOHP	3.069e-3	39.6*	1.214e-1	29.6	3.885e-3	22.8*	8.862e-2	28
FU, Berlin	3.097e-3	41.0	1.270e-1	32.6	3.457e-3	24.0	8.297e-2	30
IFU, Garmisch	3.246e-3	41.3*	1.341e-1	28-30	4.042e-3	20.3*	8.204e-2	30-33
MRI, Tsukuba	3.294e-3	35.0	1.153e-1	30	4.202e-3	20.0	8.405e-2	30
NASA, Goddard	3.514e-3	20.0	7.028e-2	35	3.795e-3	20.0	7.591e-2	32.5
NASA, Langley	3.159e-3	35.0	1.106e-1	29.8	3.764e-3	27.0	1.016e-1	29.8
NOAA, M. Loa	3.298e-3	30.0	9.893e-2	27-30			no results	
NIES, Tsukuba	3.042e-3	40.0	1.217e-1	29	3.894e-3	25.0	9.735e-2	29.5
U, LAquila	3.151e-3	40.0	1.261e-1	27-30	3.821e-3	25.0	9.633e-2	27-30
YORK, Toronto	3.382e-3	43.4*	1.468e-1	28-32	3.952e-3	30.7*	1.213e-1	27-33
Average	3.226e-3	37.1	1.191e-1		3.849e-3	25.8	9.810e-2	
StdDev	1.537e-4	6.2	1.866e-2		3.589e-4	5.7	1.652e-2	
StdDev [%]	5%	17%	16%		9%	22%	17%	

* For DWD, IFU, YORKU and CNR at 532 nm α/β varies with altitude - in the table the ratio between optical density and integrated backscatter is given.

D, Ho-
neutral
s were
80 km
f high
rences
id 532
ces, at
causes
m the
tively.
do not

it Dis-
turns.
variable
is and
.

β [sr],

92

z_0

5-29

4-40

?9.3

28

30

0-33

33

12.5

?9.8

7-30

7-33

table

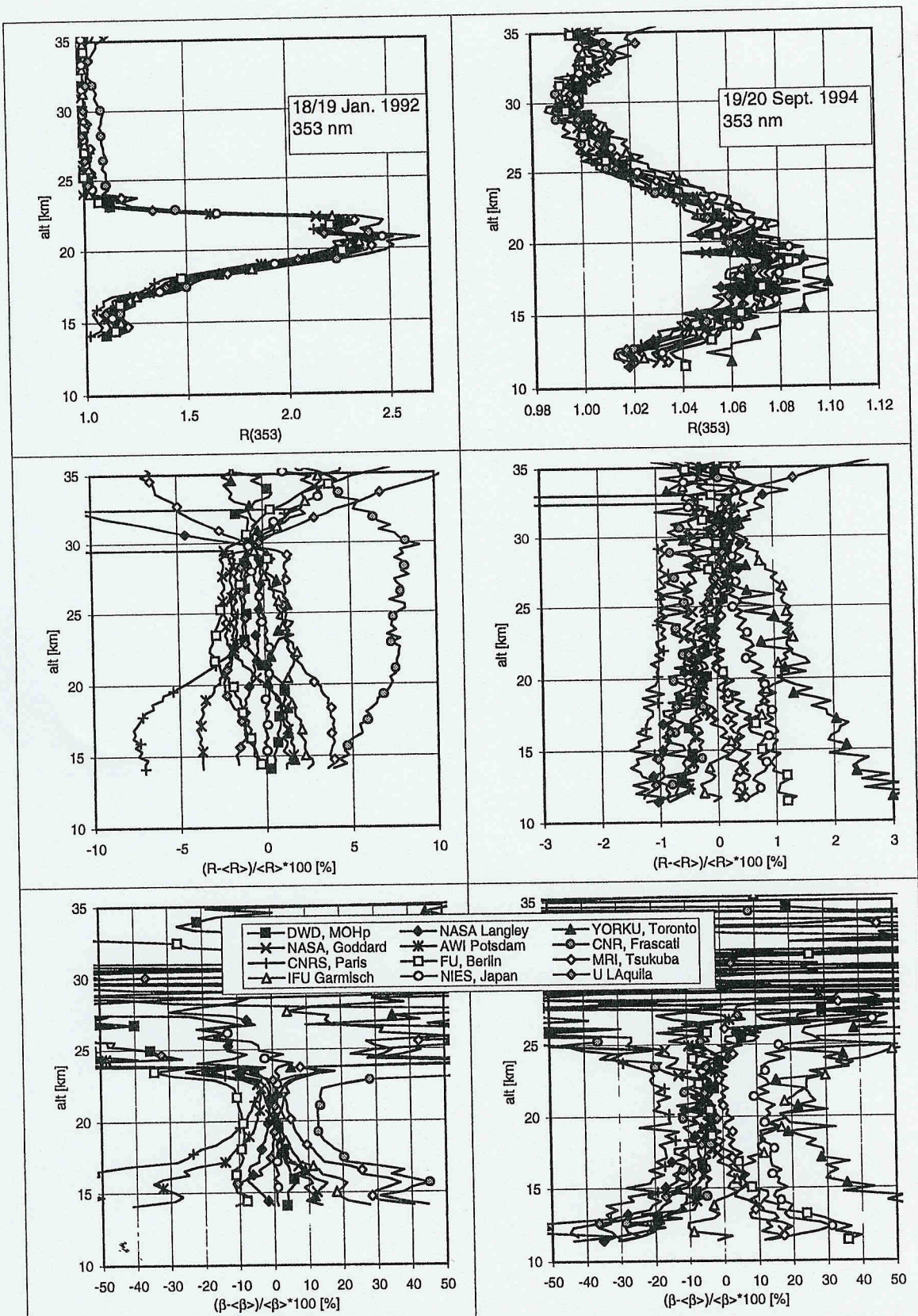


Fig. 1. Results of the intercomparison at 353 nm. Left panels: 18/19 January 1992. Right panels: 19/20 September 1994. Top panels: Scattering ratio R . Middle panels: Relative differences to average scattering ratio $\langle R \rangle$. Bottom panels: Relative differences of aerosol backscatter coefficient β to the average $\langle \beta \rangle$ of all groups.

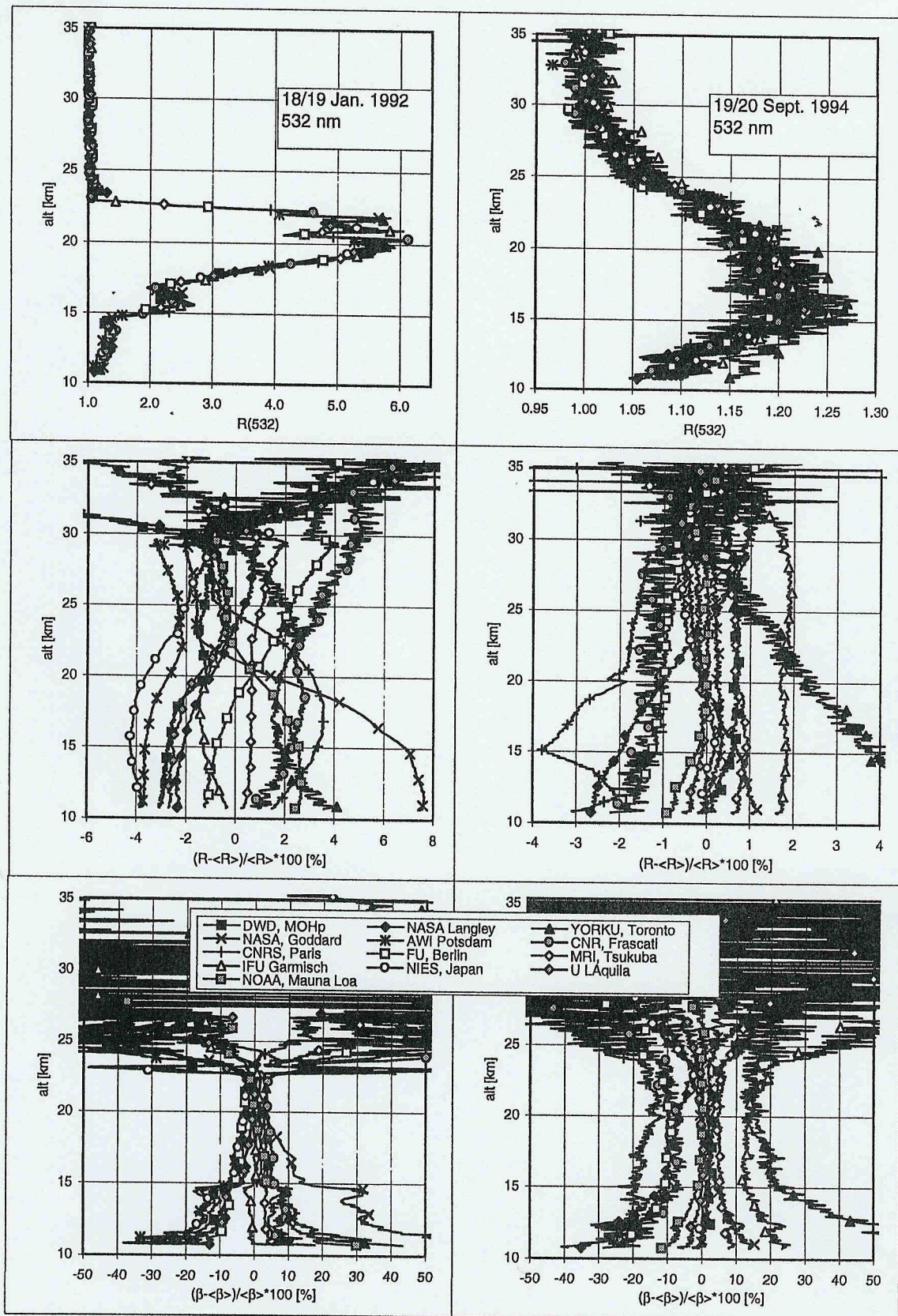


Fig. 2. Same as Figure 1, but for 532 nm.